

A Novel Method of ^{18}F Radiolabeling for PET

William J. McBride¹, Robert M. Sharkey², Habibe Karacay², Christopher A. D'Souza¹, Edmund A. Rossi³, Peter Laverman⁴, Chien-Hsing Chang^{1,3}, Otto C. Boerman⁴, and David M. Goldenberg²

¹Immunomedics, Inc., Morris Plains, New Jersey; ²Center for Molecular Medicine and Immunology, Garden State Cancer Center, Belleville, New Jersey; ³IBC Pharmaceuticals, Inc., Morris Plains, New Jersey; and ⁴Radboud University Nijmegen Medical Centre, Nijmegen, The Netherlands

Small biomolecules are typically radiolabeled with ^{18}F by binding it to a carbon atom, a process that usually is designed uniquely for each new molecule and requires several steps and hours to produce. We report a facile method wherein ^{18}F is first attached to aluminum as Al^{18}F , which is then bound to a chelate attached to a peptide, forming a stable Al^{18}F -chelate-peptide complex in an efficient 1-pot process. **Methods:** For proof of principle, this method was applied to a peptide suitable for use in a bispecific antibody pretargeting method. A solution of $\text{AlCl}_3 \cdot 6\text{H}_2\text{O}$ in a pH 4.0 sodium-acetate buffer was mixed with an aqueous solution of ^{18}F to form the Al^{18}F complex. This was added to a solution of IMP 449 (NOTA-*p*-Bn-CS-D-Ala-D-Lys(HSG)-D-Tyr-D-Lys(HSG)-NH₂) (NOTA-*p*-Bn-CS is made from S-2-(4-isothiocyanatobenzyl)-1,4,7-triazacyclononane-1,4,7-triacetic acid; HSG is histamine-succinyl-glycine) and heated to 100°C for 15 min. In vitro and in vivo stability and targeting ability of the Al^{18}F -IMP 449 were examined in nude mice bearing LS174T human colonic tumors pretargeted with an anti-CEACAM5 bispecific antibody (TF2). **Results:** The radiolabeled peptide was produced in 5%–20% yield with an estimated specific activity of 18,500–48,100 GBq (500–1,300 Ci)/mmol. The Al^{18}F -IMP 449 was stable for 4 h in serum in vitro, and in animals, activity isolated in the urine 30 min after injection was bound to the peptide. Nonchelated Al^{18}F had higher tissue uptake, particularly in the bones, than the chelated Al^{18}F -IMP 449, which cleared rapidly from the body by urinary excretion. Tumor uptake was 30-fold higher with TF2-pretargeted Al^{18}F -IMP 449 than with the peptide alone. Dynamic PET showed tumor localization within 30 min and rapid and thorough clearance from the body. **Conclusion:** The ability to bind highly stable Al^{18}F to metal-binding ligands is a promising new labeling method that should be applicable to a diverse array of molecules for PET.

Key Words: bispecific antibody; cancer; CEACAM5; ^{18}F ; pretargeting; molecular imaging; PET

J Nucl Med 2009; 50:991–998

DOI: 10.2967/jnumed.108.060418

PET has become one of the most prominent functional imaging modalities in diagnostic medicine, with high sensitivity (fmol), high resolution (e.g., 4–10 mm), and

tissue accretion that can be adequately quantitated (1). Although ^{18}F -FDG is the most widely used functional imaging agent in oncology (2), there is a keen interest in developing other labeled compounds for functional imaging to complement and augment anatomic imaging methods (3), especially with hybrid PET/CT systems. Thus, a facile method of conjugating positron-emitting radionuclides to various molecules is needed.

Although there are several PET radionuclides, ^{18}F (β^+ , 0.635 MeV [97%]; half-life, 110 min) has nearly ideal properties for PET, such as low positron energy, lack of side emissions, and a suitable half-life. Peptides and other small molecules are excellent candidates for use as ^{18}F -labeled agents, because they have similar properties to FDG (i.e., they rapidly enter the extracellular space from the blood, where they are accessible to the cells and then clear just as quickly from the body). However, preparing ^{18}F -conjugates can be an arduous and lengthy process, particularly given the short half-life (110 min) of ^{18}F . For example, peptides are conventionally labeled with ^{18}F in a 2- or 3-step process involving the labeling and purification of a small molecule (prosthetic group) and subsequent conjugation/purification of the conjugate (4). The first step typically involves the purification of ^{18}F , and the second usually follows the path established for the production of ^{18}F -FDG (5). The purified ^{18}F is mixed with potassium carbonate, a crown-ether (Kryptofix 222; Merck), and boiled to dryness. The sample is then azeotropically dried twice with acetonitrile. Subsequently, the ^{18}F is attached to a prosthetic group, which is present in great excess compared with the moles of ^{18}F . The radiolabeled prosthetic group should be purified; the prosthetic group is then conjugated to the desired targeting molecule, and the product is purified again to obtain a radiolabeled targeting agent with high specific activity. Some examples include succinyl ^{18}F fluoro-benzoate (6–8), 4- ^{18}F -fluorobenzaldehyde (9–12), other acyl compounds (13–16), or click chemistry adducts (17). The total synthesis and formulation time for these methods ranges between 1 and 3 h, with most of the time dedicated to the high-performance liquid chromatography (HPLC) purification of the labeled peptides to obtain the specific activity required for in vivo targeting.

Since fluoride binds to most metals (18–20), we speculated that an ^{18}F -metal complex could be bound to a chelate on a

Received Nov. 18, 2008; revision accepted Mar. 18, 2009.
For correspondence or reprints contact: William J. McBride,
Immunomedics, Inc., 300 American Way, Morris Plains, NJ 07950.
E-mail: bmcbride@immunomedics.com
COPYRIGHT © 2009 by the Society of Nuclear Medicine, Inc.

targeting agent in a similar manner to most radiometal-labeling procedures for antibodies and peptides—procedures that are typically accomplished within 15 min and with quantitative yields. Because we have reported previously the synthesis of several synthetic hapten-conjugated peptides that contain a variety of chelating groups for binding radiometals used for in vivo targeting of cancer with a bispecific antibody (BsmAb) pretargeting system (21–24), this system was selected as a testing platform for evaluating Al¹⁸F peptides. This procedure has been shown to be highly sensitive and specific for detecting cancers in humans (25), and animal testing has shown improved and more rapid tumor visualization than has been possible with directly radiolabeled antibodies, even providing more sensitive imaging than ¹⁸F-FDG in animal studies (26,27).

In this report, we describe our initial work leading to the discovery of a suitably stable first-generation ligand that is capable of binding the Al¹⁸F complex to a hapten-peptide. When used in a pretargeting setting, the pretargeted ¹⁸F-hapten-peptide was stable and provided excellent tumor localization within 1 h.

MATERIALS AND METHODS

Reagents

The *p*-SCN-Bn-NOTA was purchased from MacroCyclics, Inc.; protected amino acids, other peptide synthesis reagents, and resins from Creosalus, Chem Impex, Bachem, PepTech Corp., and EMD Biosciences; aluminum chloride hexahydrate from Sigma-Aldrich; and other solvents and reagents from Fisher Scientific or Sigma-Aldrich. The analytic and preparative reverse-phase HPLC (RP-HPLC) columns were purchased from Phenomenex or Waters Corp., and size exclusion HPLC (SE-HPLC) columns from BioRad. ¹⁸F and FDG were supplied by IBA Molecular.

The recombinant, humanized, tri-Fab BsmAb, TF2, was provided by IBC Pharmaceuticals, Inc. TF2 binds divalently to carcinoembryonic antigen (CEACAM5, CEA, CD66e) and monovalently to the synthetic hapten, HSG (histamine-succinyl-glycine) (28). The BsmAb was more than 95% immunoreactive against CEACAM5 and the divalent-HSG NOTA-peptide, IMP 449, using a SE-HPLC method described previously (28).

Preparation of Chelate-Hapten-Peptide

IMP 272 (DTPA-Gln-Ala-Lys(HSG)-D-Tyr-Lys(HSG)-NH₂, MH⁺ 1,512), IMP 375 (DTPA-Dpr((R)-3-amino-3-(2-bromophenyl)-propionyl)-D-Ala-D-Lys(HSG)-D-Ala-D-Lys(HSG)-NH₂), and IMP 449 (NOTA-*p*-Bn-NH-CS-D-Ala-D-Lys(HSG)-D-Tyr-D-Lys(HSG)-NH₂, MH⁺ 1,459) were prepared as described previously (29,30).

Preparation of IMP 449 Labeling Kits

The peptide, IMP 449, was formulated with the addition of ascorbic acid. For this, 8 mg of lyophilized IMP 449 (5.48 μmol) were mixed with 0.1549 g of L-(+)-ascorbic acid and dissolved in 10.5 mL of deionized water. The liquid was dispensed in 1.0-mL aliquots into 2-mL lyophilization vials. The solutions were frozen, lyophilized, and sealed under vacuum.

Preparation of Al¹⁸F

AlCl₃ hexahydrate was used to prepare a 2 mM Al³⁺ stock solution in a 0.1 M pH 4 sodium acetate buffer. Al¹⁸F was

prepared using a 3-μL (6 nmol) aliquot of the aluminum stock solution, which was mixed with 50 μL of the ¹⁸F received from the commercial supplier (e.g., 370 MBq [10 mCi] in ~0.5 mL of water). This Al¹⁸F was used for the preparation of IMP 272, but later, we purified the ¹⁸F to remove contaminating metals that might otherwise compete for binding to the chelates (31). Briefly, a Sep-Pak Light Accell Plus QMA cartridge (Waters) was washed with 10 mL of 0.4 M KHCO₃ followed by 10 mL of deionized water. ¹⁸F, received in 2 mL of water (~1.48 GBq [40 mCi]), was loaded onto the cartridge. The cartridge was washed with 5 mL of deionized water. ¹⁸F was then eluted from the cartridge in 0.2-mL fractions with 0.4 M KHCO₃. Most of the activity was in the second 0.2-mL fraction. Three microliters (6 nmol) of the stock aluminum acetate solution were added to this fraction, which was then added to IMP 449.

¹⁸F Radiolabeling of IMP 272

Three microliters of a 2 mM IMP 272 stock solution in 0.1 M acetate buffer solution, pH 4.0, were added to the Al¹⁸F mixture (53 μL) prepared using the unpurified ¹⁸F. This was placed in a heating block at 110°C for 15 min and analyzed by RP-HPLC on a Gemini 5-μm C18110 A, 250 × 4.60 mm, column (Phenomenex) using 0.1% NH₄OAc buffers (flow rate: 1 mL/min; buffer A: 0.1% NH₄OAc in water; buffer B: 0.1% NH₄OAc in 90% acetonitrile, 10% water; gradient: 100% buffer A to 100% buffer B over 30 min). Because the initial HPLC analysis showed poor incorporation, an additional 10 μL of the IMP 272 stock solution were added, and it was heated again and analyzed by RP-HPLC.

¹⁸F Radiolabeling of IMP 449

The Al¹⁸F solution prepared from the purified ¹⁸F was injected into the lyophilized IMP 449 vial and then heated at 100°C for 15 min. The reaction solution was RP-HPLC-purified using a monolithic C-18 column (100 × 4.5 mm; Phenomenex) under the following conditions: flow rate: 3 mL/min; buffer A: 0.1% trifluoroacetic acid (TFA) in deionized water; buffer B: 0.1% TFA in 90% acetonitrile; gradient: 100% buffer A to 75% buffer A/25% buffer B over 15 min using a linear gradient. The HPLC eluent was collected with a fraction collector in 30-s increments. Unbound ¹⁸F and Al¹⁸F are eluted in the void volume. As the gradient proceeds, the Al¹⁸F IMP 449 is eluted first, followed by the unlabeled IMP 449 about 1 min later. Any Al-IMP 449 (without ¹⁸F) coelutes with the Al¹⁸F IMP 449. The fraction containing the Al¹⁸F IMP 449 was diluted with water and loaded onto an Oasis 1-mL hydrophilic-lipophilic-balanced (HLB) column (part number 186001879; Waters). The HLB column was washed with three 1-mL aliquots of water to remove the acetonitrile and TFA. The labeled peptide was then eluted with 2 × 200 μL of 1:1 EtOH:H₂O into a vial containing 15 mg of ascorbic acid neutralized to pH 6.6 with NaOH.

To estimate the specific activity of the labeled products, we assumed that the specific activity of ¹⁸F is approximately 370 TBq (10,000 Ci)/mmol (the theoretic specific activity of ¹⁸F is about 62,900 TBq/mmol, but because of ¹⁹F contamination it is generally considered to be the lower assumed value). The specific activity of the labeled peptide is controlled by the amount of aluminum that is added to the labeling reaction, since ¹⁸F will not bind to the peptide without the metal. As an example, in one study, 4.4 GBq, or 1.2 × 10⁻⁵ mmol of total fluoride, was added to 6 × 10⁻⁶ mmol of the aluminum solution, which was added to 5.2 × 10⁻⁴ mmol of peptide. The crude reaction mixture was purified to obtain 329 MBq in 2 main fractions (201 and 128 MBq). The 201-

MBq fraction was then further purified on an HLB column to remove the acetonitrile and TFA, resulting in a final product yield of 174.6 MBq. It is assumed that each fraction contained the same amount of the Al-IMP 449, so since the 201-MBq fraction contained 60.6% of the labeled peptide, it is also assumed that it contained 60% of the aluminum added or 3.63×10^{-6} mmol of the aluminum peptide; therefore, the theoretic specific activity of the labeled peptide is $0.1746 \text{ GBq}/3.63 \times 10^{-6} \text{ mmol} = 48,100 \text{ GBq}$ (1,300 mCi)/mmol.

Al¹⁸F IMP 449

A 960- μL aliquot of a 0.02 M solution of $\text{AlCl}_3 \cdot 6\text{H}_2\text{O}$ in 0.5 M NaOAc, pH 4, was mixed with 192 μL of NaF in 0.5 M NaOAc, pH 4. The solution was added to 0.0280 g (MH^+ 1,459; 1.919×10^{-5} mol) of IMP 449, heated in a 100°C heating block for 17 min, and then purified by RP-HPLC using a 30×150 mm Sunfire C-18 column (Waters) eluting with 0.01% ammonium acetate buffers. The HPLC buffers were as follows: buffer A, 0.1% NH_4OAc in H_2O , and buffer B, 0.1% NH_4OAc 90% CH_3CN 10% H_2O . The HPLC gradient went from 100% A to 80:20 A:B over 80 min with a flow rate of 45 mL/min. The HPLC fractions were collected and lyophilized to obtain the aluminum-NOTA-IMP 449 complex, 0.0068 g, MH^+ 1,482.6534 ($\text{C}_{66}\text{H}_{92}\text{N}_{19}\text{O}_{17}\text{S}_1\text{Al}_1$, theoretic 1,482.6527), and 2 aluminum fluoride IMP 449 complexes: RT 9.73 min, 0.0106 g, MH^+ 1,502.6614 ($\text{C}_{66}\text{H}_{93}\text{N}_{19}\text{O}_{17}\text{S}_1\text{Al}_1\text{F}_1$, theoretic 1,502.6589) and RT 9.90 min, 0.0068 g, MH^+ 1,502.6588 ($\text{C}_{66}\text{H}_{93}\text{N}_{19}\text{O}_{17}\text{S}_1\text{Al}_1\text{F}_1$, theoretic 1,502.6589).

Stability Testing

Al¹⁸F-IMP 449 (1,850 kBq [50 μCi], 50 μL) was added to 0.5 mL of freshly collected and sterile-filtered human serum. The sample was incubated at 37°C in a humidified 5% CO_2 incubator. At approximately 1 and 4 h, the sample was analyzed by RP-HPLC, as well as by SE-HPLC after mixing with TF2 to determine the percentage immunoreactivity with HSG. HPLC systems were equipped with in-line ultraviolet and radiation detectors. A Bio-Sil SE 250 column (Bio-Rad Laboratories, Inc.) attached to a guard column was eluted with a buffer containing 0.2 M sodium phosphate, 0.02% sodium azide, and 10 mM ethylenediaminetetraacetic acid, pH 7.0. RP-HPLC studies were performed on an RCM 8×10 C18 NovaPak (4- μM) column (Waters), eluted using a gradient of 100% solvent A to 45% solvent B, 55% solvent A in 15 min, then at 100% B for 5 min before equilibration to initial conditions. The flow rate was 1.5 mL/min, solvent A was 0.075% TFA in H_2O , and B was 0.075% TFA in 75% CH_3CN and 25% H_2O .

In vivo stability was examined by injecting 18.5 MBq of Al¹⁸F-IMP 449 intravenously to 3 non-tumor-bearing mice, and then 30 min later, the animals were anesthetized, bled, and then necropsied to remove urine from the urinary bladder. Samples were analyzed by RP- and SE-HPLC.

Biodistribution and Small-Animal PET

All studies were performed with the approval of the institutional animal care and use committee. The human colonic cancer cell line, LS174T (ATCC), was implanted subcutaneously in 6-wk-old NCr *v-m* female nude mice (Taconic). When tumors were visible, 162 μg (~ 1 nmol/0.1 mL) of TF2 were injected intravenously in pretargeted animals, and then 16–18 h later, about 0.1 nmol of Al¹⁸F-IMP 449 (3.11 MBq [84 μCi]/0.1 mL) was injected intravenously. Other nonpretargeted control animals received ¹⁸F alone (5.5 MBq [150 μCi]), Al¹⁸F complex alone (5.55 MBq [150 μCi]), the Al¹⁸F-IMP 449 peptide alone (3.11 MBq [84 μCi]), or ¹⁸F-FDG (5.55 MBq

[150 μCi]). ¹⁸F and ¹⁸F-FDG were obtained on the day of use. Animals receiving ¹⁸F-FDG were kept fasting overnight, but water was given ad libitum.

At 1.5 h after the radiotracer injection, the animals were anesthetized, bled intracardially, and necropsied. Tissues were weighed and counted together with a standard dilution prepared from each of the respective products. Because of the short physical half-life of ¹⁸F, standards were interjected between each group of tissues from each animal. Uptake in the tissues is expressed as the counts per gram divided by the total injected activity to derive the percentage injected dose per gram.

Two types of imaging studies were performed. In one set, 3 nude mice bearing small LS174T subcutaneous tumors received either the pretargeted Al¹⁸F-IMP 449, Al¹⁸F-IMP 449 alone (not pretargeted) (both forms: 135 μCi [5 MBq]; 0.1 nmol), or ¹⁸F-FDG (5 MBq [135 μCi]). At 2 h after the intravenous radiotracer injection, the animals were anesthetized with a mixture of $\text{O}_2/\text{N}_2\text{O}$ and isoflurane (2%) and kept warm during the scan. The mice were placed supine on the bed of an Inveon animal PET scanner (Siemens Preclinical Solutions). This scanner has an intrinsic spatial resolution of 1.5 mm. Emission scans were acquired over 15 min (¹⁸F-FDG) or 30 min (Al¹⁸F-IMP 449). Scans were reconstructed using Inveon Acquisition Workplace software (IAW, version 1.2) using an ordered-set expectation maximization 3-dimensional/maximum a posteriori (OSEM3D/MAP) algorithm with the following parameters: matrix, $256 \times 256 \times 159$; pixel size, $0.43 \times 0.43 \times 0.8$ mm; and MAP prior of 0.5 mm. Representative coronal cross-sections (0.8 mm thick) in a plane located approximately in the center of the tumor were displayed, with intensities adjusted until pixel saturation occurred in any region of the body (excluding the bladder) and without background adjustment.

In a separate dynamic imaging study, a single LS174T-bearing nude mouse that was given the TF2 BsmAb 16 h earlier was anesthetized with a mixture of $\text{O}_2/\text{N}_2\text{O}$ and isoflurane (2%), placed supine on the camera bed, and then injected intravenously with 8.1 MBq (219 μCi) of Al¹⁸F IMP 449 (0.16 nmol). Data acquisition was initiated immediately and continued for 120 min. Data were graphed in 24 frames of 5 min each. The scans were reconstructed using OSEM3D/MAP with the same parameters as described above. Each of the 24-image time frames was examined. For presentation, time frames ending at 5, 15, 30, 60, 90, and 120 min (i.e., the 5-min image is for the period from time zero to 5 min) were displayed for each cross-section (coronal, sagittal, and transverse). For sections containing tumor, at each interval the image intensity was adjusted until pixel saturation first occurred in the tumor. Image intensity was increased as required over time to maintain pixel saturation within the tumor. Coronal and sagittal cross-sections without tumor taken at the same interval were adjusted to the same intensity as the transverse section containing tumor. Background activity was not adjusted.

RESULTS

Initial Test Compounds

Because diethylenetriaminepentaacetic acid (DTPA) has been used widely for binding a variety of metals, including aluminum (32), a DTPA-hapten-peptide, IMP 272, was prepared (Fig. 1). On the basis of the prior experience of Martin et al. (33), labeling was performed at approximately pH 4.0, since this was reported to be optimal for the formation of AlF_n species in water and the same pH range has been used to bind Al^{3+} to ligands (34). Under

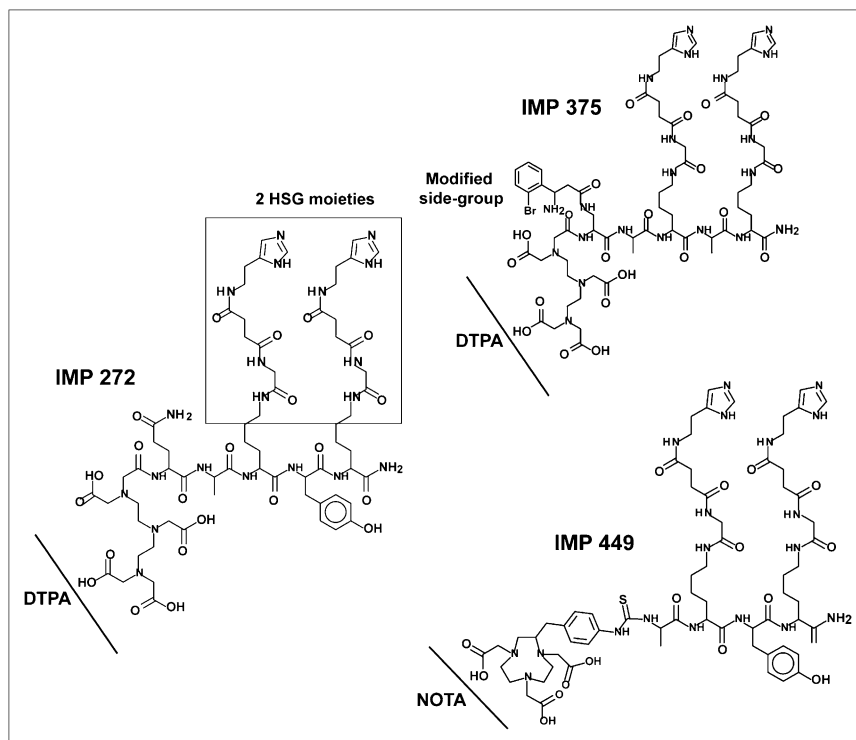


FIGURE 1. DTPA- and NOTA-HSG-hapten-peptides.

the initial reaction conditions (6 nmol of aluminum solution added to ^{18}F plus 6 nmol of IMP 272, pH 4.0; heated at 100°C for 15 min), RP-HPLC showed that only 7% of the activity was bound. However, when 26 nmol of peptide were added to this same reaction mixture and heating was continued for a further 15 min, the yield increased to 92%. Although the yields were good, the Al^{18}F -IMP 272 was unstable in water (17% loss of ^{18}F in 40 min at room temperature). Since chelates vary in their affinity for different metals, we tested other ^{18}F -metal complexes (Ga, In, Zr, Lu, and Y) for their binding to IMP 272. These complexes also bound to the peptide, but not as well as Al^{18}F , and they too were unstable in water, as is consistent with the findings of others (20,28). In an attempt to better stabilize the Al^{18}F complex, several other DTPA-hapten-peptides were synthesized by altering the residues adjacent to the DTPA. One ^{18}F -labeled peptide, IMP 375 (Fig. 1), was stable in water, with 98% radiolabeling yield, but this peptide, like the others, was not sufficiently stable in human serum *in vitro*.

Because the literature indicated that Al^{3+} binds F^- more strongly than most other metals (20,33,35), and that $\text{Al}(\text{F})_n$ complexes are stable *in vivo* (35,36), the instability of Al^{18}F on the DTPA ligand most likely is due to the weak binding of the metal complex to DTPA and not to dissociation of the AlF complex. Thus, we continued with the AlF complex but focused on new chelates to bind Al^{18}F , recognizing that the AlF complex might have binding characteristics different from what has been reported for aluminum. We tested several different chelates, such as deferoxamine, 1,4,7,10-tetraazacyclododecane-1,4,7,10-tetraacetic acid, ethylenediamine-tetraacetic acid, symmetric DTPA, phosphonates, phosphates, and 1,4,7-triazacyclononane-1,4,7-triacetic acid

(NOTA). Screening was performed by mixing ^{18}F with 6 nmol of Al^{3+} , adding 40 nmol of peptide, and heating for 15 min at 100°C . The peptides were then examined by RP-HPLC to determine the labeling yield. Labeling yields with all the other chelate hapten-peptides were lower (or not bound at all) than with DTPA, and all, except the Al^{18}F NOTA complex, were unstable in serum. Because Andre et al. (34) had reported that NOTA formed stable complexes with aluminum, this chelate was investigated further.

^{18}F Labeling of IMP 449

Initial yields of the Al^{18}F NOTA-peptide (IMP 449; Fig. 1) were only about 5% under the standard screening conditions (i.e., with 40 nmol of peptide); however, when 522 nmol of peptide were used, labeling yields increased to a range of 5%–20% (without correcting for decay) after HPLC purification. The ^{18}F -labeled peptide was produced without a drying step and with a single HPLC purification within 60 min to obtain a labeled peptide suitable for *in vivo* use. The purified product was stable in serum at 37°C for 4 h (Fig. 2A), and immunoreactivity testing also confirmed that the Al^{18}F complex was bound firmly to the peptide. As shown in Figure 2B, when mixed with an HSG-binding BsmAb, TF2, and analyzed by SE-HPLC, only the purified Al^{18}F -IMP 449 eluted at a molecular size consistent with complexes formed between TF2 and the Al^{18}F -IMP 449 di-HSG peptide, whereas ^{18}F alone and the nonchelated Al^{18}F complex continued to elute in the included volume. Thus, Al^{18}F -IMP 449 met our primary criteria that the compound should be prepared in a timely manner and have suitable stability in serum to proceed with animal testing.

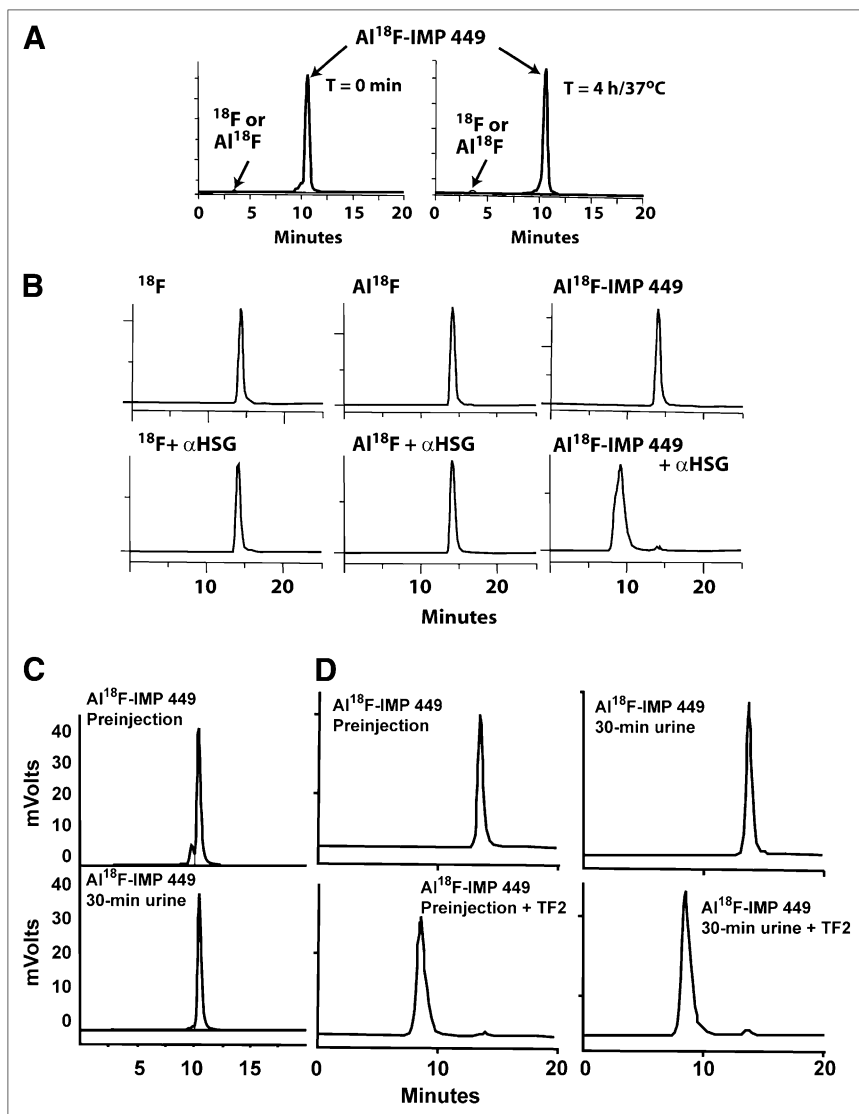


FIGURE 2. Serum stability and immunoreactivity of Al^{18}F -IMP 449. (A) RP-HPLC showing elution of purified product at start of study (left) and then 4 h later after incubation at 37°C in fresh human serum (right). (B) SE-HPLC illustrates retention of binding of di-HSG containing IMP 449 peptide after radiolabeling with Al^{18}F . Top graphs show ^{18}F alone, nonchelated Al^{18}F complex, and Al^{18}F IMP 449 eluting in total included volume of column. Bottom graphs show elution of each product after being incubated with excess amount of anti-HSG antibody for 30 min at 37°C . Only Al^{18}F IMP 449 elution profile shifted to migrate with antibody, and 100% of activity eluted at this earlier time. (C) RP-HPLC profile of Al^{18}F -IMP-449 before injection in animals (top) and then in 30-min urine sample (bottom). (D) SE-HPLC of same labeled product as in C before animal injection (left), with and without addition of TF2 to show binding to HSG. Right graphs show profiles from urine sample taken 30 min after injection.

Al^{19}F -IMP 449 Mass Spectroscopy Analysis of AIF Binding to IMP 449

The aluminum and Al^{19}F complexes of the peptide were prepared so that the complexes could be analyzed by HPLC and by mass spectroscopy to help determine the nature of the complexes formed. Two Al^{19}F complexes were formed with retention times that matched the ^{18}F complexes when examined under similar conditions. The mass of the Al^{19}F -IMP 449 MH^+ 1,502.6588 ($\text{C}_{66}\text{H}_{93}\text{N}_{19}\text{O}_{17}\text{S}_1\text{Al}_1\text{F}_1$, theoretic 1,502.6589) is consistent with a complex in which the AIF is binding 2 of the NOTA carboxyl groups and the third carboxyl is still protonated (Fig. 3). Aluminum is known to bind NOTA to form hexadentate bonds to the 3 nitrogens and 3 carboxyls (34). Thus, it appears that the AIF complex has pentadentate binding to NOTA, with the sixth binding site of the aluminum filled with the fluoride ion.

In Vivo Studies

To assess the stability of the Al^{18}F -IMP 449 in vivo, animals were given ^{18}F alone and Al^{18}F so that the tissue

distribution of each component would be known. ^{18}F alone and Al^{18}F complexes had similar uptake in all tissues, but considerable differences were found when the Al^{18}F complex was chelated to IMP 449 (Table 1). The most striking differences were found in the uptake in bone, where the nonchelated ^{18}F was 60- to nearly 100-fold higher in the scapula and approximately 200-fold higher in the spine. This distribution is expected, since ^{18}F , or even a metal-fluoride complex, is known to accrete in bone (37). Higher uptake was also observed in the tumor and intestines, as well as in muscle and blood. The chelated Al^{18}F -IMP 449 had significantly lower uptake in all the tissues except the kidneys, illustrating the ability of the chelate complex to be removed efficiently from the body by urinary excretion. Pretargeting the Al^{18}F IMP 449 using the TF2 anti-CEACAM5 BsmAb shifted uptake to the tumor, increasing it from $0.20\% \pm 0.05\%$ injected dose per gram at 1.5 h, whereas uptake in the normal tissues was similar to the Al^{18}F -IMP 449 alone. Tumor-to-nontumor ratios were 146 ± 63 , 59 ± 24 , 38 ± 15 , and 2.0 ± 1.0 for the blood, liver, lungs, and

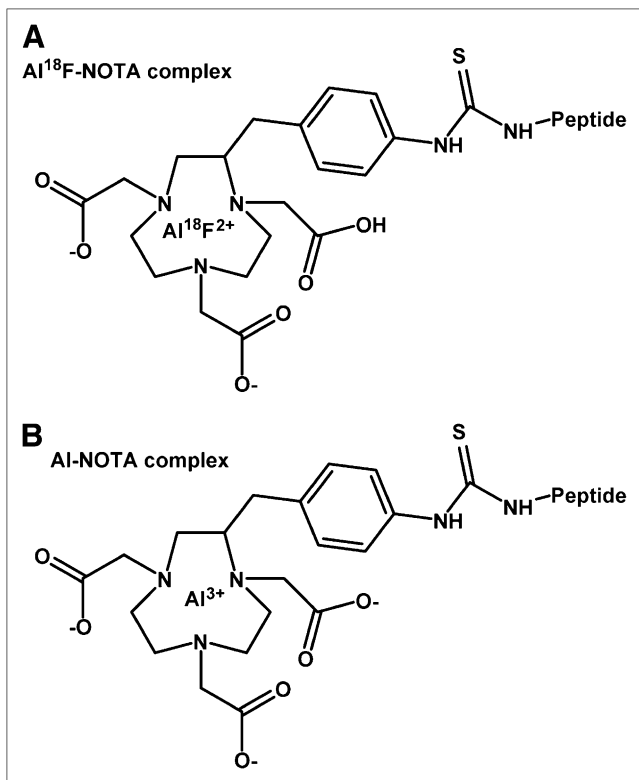


FIGURE 3. Schematic representation of Al¹⁸F-NOTA (A) and Al-NOTA (B) binding based on mass spectroscopy data of ¹⁹F-IMP 449 complex.

kidneys, respectively, with other tumor-to-tissue ratios being greater than 100:1 at this time. Although both ¹⁸F alone and Al¹⁸F alone had higher uptake in the tumor than did the chelated Al¹⁸F-IMP 449, yielding tumor-to-blood ratios of

6.7 ± 2.7 and 11.0 ± 4.6 vs. 5.1 ± 1.5, respectively, tumor uptake and tumor-to-blood ratios were significantly increased with pretargeting (all *P* values < 0.01).

Tissue distribution of the Al¹⁸F-IMP 449 was also compared with ¹⁸F-FDG (Table 1). ¹⁸F-FDG uptake was appreciably higher than Al¹⁸F-IMP 449 uptake in all normal tissues, except the kidneys. Uptake in tumor was similar for both the pretargeted Al¹⁸F-IMP 449 and ¹⁸F-FDG, but because of the higher accretion of ¹⁸F-FDG in most normal tissues, tumor-to-nontumor ratios with ¹⁸F-FDG were significantly lower than those in the pretargeted animals (all *P* values < 0.001).

We attempted to examine the stability of the Al¹⁸F-IMP 449 in the blood from several animals given the peptide alone, but because the peptide cleared so quickly, there was insufficient activity for HPLC analysis with samples collected just 30 min after injection. However, analysis of the activity eliminated in the urine of these animals showed that all of it was associated with the peptide, and in fact, the activity in the urine also shifted on a SE-HPLC column when TF2 was added, indicating that the peptide retained at least one of its HSG moieties (Figs. 2C and 2D). Collectively, these data indicate that ¹⁸F remained firmly attached to the aluminum, and the Al¹⁸F complex bound to NOTA-IMP 449 was stable in vivo.

Several animals were imaged to analyze the biodistribution of Al¹⁸F IMP 449 alone or Al¹⁸F-IMP 449 pretargeted with TF2, as well as ¹⁸F-FDG. Static images initiated at 2.0 h after the radioactivity had been injected corroborated the previous tissue distribution data, showing uptake almost exclusively in the kidneys (Fig. 4). A 21-mg tumor was easily visualized in the pretargeted animal, whereas the animal given the Al¹⁸F-IMP 449 alone failed to localize the tumor, having only renal uptake. No evidence of bone

TABLE 1. Biodistribution of TF2-Pretargeted Al¹⁸F-IMP 449 and Other Control ¹⁸F-Labeled Agents in Nude Mice Bearing LS174T Human Colonic Cancer Xenografts

Site	%ID/g (mean ± SD) 1.5 h after injection				
	¹⁸ F alone	Al ¹⁸ F alone	Al ¹⁸ F-IMP 449 alone	TF2-pretargeted Al ¹⁸ F-IMP 449	¹⁸ F-FDG
Tumor	1.02 ± 0.45	1.38 ± 0.39	0.20 ± 0.05	6.01 ± 1.72	7.25 ± 2.54
Liver	0.11 ± 0.02	0.12 ± 0.02	0.08 ± 0.03	0.11 ± 0.03	1.34 ± 0.36
Spleen	0.13 ± 0.06	0.10 ± 0.03	0.08 ± 0.02	0.08 ± 0.02	2.62 ± 0.73
Kidney	0.29 ± 0.07	0.25 ± 0.07	3.51 ± 0.56	3.44 ± 0.99	1.50 ± 0.61
Lung	0.26 ± 0.08	0.38 ± 0.19	0.11 ± 0.03	0.17 ± 0.04	3.72 ± 1.48
Blood	0.15 ± 0.03	0.13 ± 0.03	0.04 ± 0.01	0.04 ± 0.02	0.66 ± 0.19
Stomach	0.21 ± 0.13	0.15 ± 0.05	0.20 ± 0.32	0.12 ± 0.18	2.11 ± 1.04
Small intestine	1.53 ± 0.33	1.39 ± 0.34	0.36 ± 0.23	0.27 ± 0.10	1.77 ± 0.61
Large intestine	1.21 ± 0.13	1.78 ± 0.70	0.05 ± 0.04	0.03 ± 0.01	2.90 ± 0.79
Scapula	6.13 ± 1.33	9.83 ± 2.31	0.08 ± 0.06	0.04 ± 0.02	10.63 ± 5.88
Spine	19.88 ± 2.12	19.03 ± 2.70	0.13 ± 0.14	0.08 ± 0.03	4.21 ± 1.79
Muscle	0.16 ± 0.05	0.58 ± 0.36	0.06 ± 0.05	0.10 ± 0.20	4.35 ± 3.01
Brain	0.15 ± 0.06	0.13 ± 0.03	0.01 ± 0.01	0.01 ± 0.00	10.71 ± 4.53
Tumor weight (g)	0.29 ± 0.07	0.27 ± 0.10	0.27 ± 0.08	0.33 ± 0.11	0.25 ± 0.21
<i>n</i>	6	7	8	7	5

%ID = percentage injected dose.
For pretargeting, animals were given TF2 16 h before injection of Al¹⁸F-IMP 449. All injections were administered intravenously.

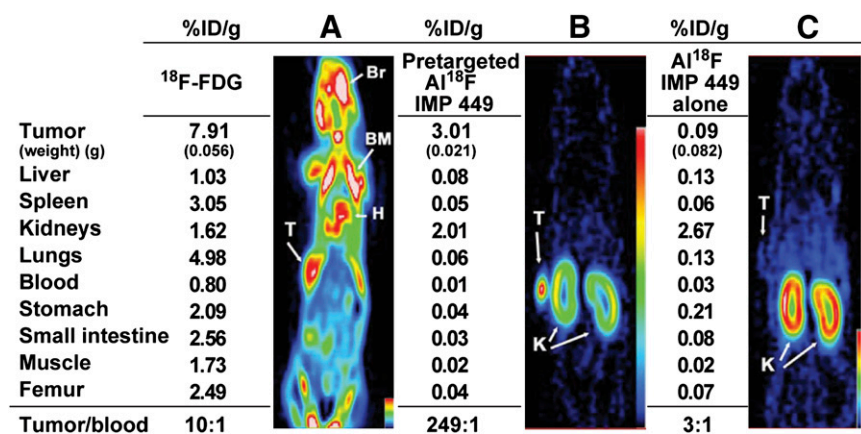


FIGURE 4. Biodistribution of ¹⁸F-labeled agents in tumor-bearing nude mice by small-animal PET. Coronal slices of 3 nude mice bearing small, subcutaneous LS174T tumor on each left flank after being injected with either ¹⁸F-FDG (A), AI¹⁸F-IMP 449 pretargeted with anti-CEA × anti-HSG BsmAb (B), or AI¹⁸F-IMP 449 alone (not pretargeted with BsmAb) (C). Biodistribution data expressed as percentage injected dose per gram (%ID/g) are given for tissues removed from animals at conclusion of imaging session. Br = brain; BM = bone marrow; H = heart; K = kidney; T = tumor.

accretion was observed, suggesting that the AI¹⁸F was bound firmly to IMP 449. This was confirmed in another pretargeted animal that underwent a dynamic imaging study monitoring the distribution of the AI¹⁸F IMP 449 at 5-min intervals over 120 min (Supplemental Fig. 1; supplemental materials are available online only at <http://jnm.snmjournals.org>). Coronal and sagittal slices showed primarily cardiac, renal, and some hepatic uptake over the first 5 min, but heart and liver activity decreased substantially over the next 10 min, whereas the kidneys remained prominent throughout the study. There was no evidence of activity in the intestines or bone over the full 120-min scan. Uptake in a 35-mg LS174T tumor was first observed at 15 min, and by 30 min, the signal was clearly delineated from background, with intense tumor activity being prominent during the entire 120-min scan.

In comparison, static images from an animal given ¹⁸F-FDG showed the expected pattern of radioactivity in the bone, heart muscle, and brain observed previously (26,27), with considerably more background activity in the body (Fig. 4). Tissue uptake measured in the 3 animals necropsied at the conclusion of the static imaging study confirmed much higher tissue ¹⁸F radioactivity in all tissues. Although tumor uptake with ¹⁸F-FDG was higher in this animal than in the pretargeted one, tumor-to-blood ratios were more favorable for pretargeting, and with much less residual activity in the body, tumor visualization was enhanced by pretargeting.

DISCUSSION

The preparation of fluorinated compounds has historically required specialized chemistries that can be cumbersome and time-consuming. We hypothesized that it might be possible to bind ¹⁸F to compounds by first creating a metal-AI¹⁸F complex that could then be attached to the compound through a metal-binding ligand. Indeed, radiolabeling of chelate-conjugated peptides and proteins with radiometals has been practiced for over 25 y (38), and thus it seemed feasible that a similar approach might be possible with a metal-¹⁸F complex, particularly because ¹⁸F can form stable complexes with several metals.

Our investigation indicated that the AI¹⁸F complex is indeed stable, but the more arduous task was finding a suitable linker for stable binding to various compounds. Several of the more commonly used chelating agents were examined, but although some would capture AI¹⁸F (even quantitatively), most were not sufficiently stable for in vivo applications. NOTA provided the first indication that the AI¹⁸F complex could be bound stably. Mass spectroscopy analysis suggests that the AI¹⁸F complex is held in place by the 3 nitrogens and 2 of the carboxyl groups. It is also important to note that while the labeling process reported here added a preformed AI¹⁸F complex to the chelate-peptide, we also were able to bind ¹⁸F to aluminum that was preloaded in the NOTA-IMP 449 (not shown).

Although yields were within the range found with conventional ¹⁸F labeling procedures, further studies are needed to select the coordination chemistries that optimize yields while retaining the stability found with this lead NOTA derivative. Nevertheless, these studies lay the foundation for a new, simplified ¹⁸F-labeling method that could allow many more compounds to be prepared with ¹⁸F PET tracer.

The labeling method described here does not require a dry-down for the ¹⁸F and is a major time-saving advantage over existing methods. The yields reported here are similar to many of the reported procedures but less than those reported for the click chemistry method (17). However, we believe that we will be able to enhance the radiolabeling yield by modifying the NOTA ligand to improve the binding kinetics of the ligand, thus possibly increasing the labeling yield while reducing the amount of peptide needed for the labeling. If the binding kinetics were to be improved sufficiently, it might be possible to eliminate the need for HPLC purification and make an ¹⁸F kit that labels in the same manner as the radiometals.

CONCLUSION

To our knowledge, this is the first report describing a direct, facile, and rapid method (60 min of total preparation time) of binding ¹⁸F via an aluminum conjugate. Although the feasibility of this approach was shown with a hapten-peptide used

for pretargeting, we have recently extended our findings to include other receptor-binding peptides and other binding ligands with improved yields, which will be reported in the future.

ACKNOWLEDGMENTS

We thank Dion Yeldell, Jayson Jebsen, Christine Johnson, Ali Mostafe, Maarten Brom, and Eric P. Visser for their technical assistance. This work was funded in part by NIH grant 1 R43 EB003751-01A1 from the National Institute of Biomedical Imaging and Bioengineering. All authors except Drs. Karacay, Sharkey, Boerman, and Laverman declare a financial interest in Immunomedics, Inc., either through employment, stock, or patents. This work was presented in part at the 55th annual meeting of the Society of Nuclear Medicine, New Orleans, Louisiana, June 15–18, 2008.

REFERENCES

1. Volkow ND, Mullani NA, Bendriem B. Positron emission tomography instrumentation: an overview. *Am J Physiol Imaging*. 1988;3:142–153.
2. Fletcher JW, Djulbegovic B, Soares HP, et al. Recommendations on the use of ^{18}F -FDG PET in oncology. *J Nucl Med*. 2008;49:480–508.
3. Torigian DA, Huang SS, Houseni M, Alavi A. Functional imaging of cancer with emphasis on molecular techniques. *CA Cancer J Clin*. 2007;57:206–224.
4. Wester HJ, Schottelius M. Fluorine-18 labeling of peptides and proteins. *Ernst Schering Res Found Workshop*. 2007;(62):79–111.
5. Hamacher K, Coenen HH, Stocklin G. Efficient stereospecific synthesis of no-carrier-added 2- ^{18}F -fluoro-2-deoxy-D-glucose using aminopolyether supported nucleophilic substitution. *J Nucl Med*. 1986;27:235–238.
6. Vaidyanathan G, Zalutsky MR. Labeling proteins with fluorine-18 using N-succinimidyl 4- ^{18}F fluorobenzoate. *Int J Rad Appl Instrum B*. 1992;19:275–281.
7. Lang L, Eckelman WC. One-step synthesis of ^{18}F labeled ^{18}F -N-succinimidyl 4-(fluoromethyl)benzoate for protein labeling. *Appl Radiat Isot*. 1994;45:1155–1163.
8. Guhlke S, Coenan H, Stöcklin G. Fluoroacylation agents based on small n.c.a. ^{18}F fluorocarboxylic acids. *Appl Radiat Isot*. 1994;45:715–727.
9. Glaser M, Morrison M, Solbakken M, et al. Radiosynthesis and biodistribution of cyclic RGD peptides conjugated with novel ^{18}F fluorinated aldehyde-containing prosthetic groups. *Bioconjug Chem*. 2008;19:951–957.
10. Poethko T, Schottelius M, Thumshirn G, et al. Two-step methodology for high-yield routine radiohalogenation of peptides: ^{18}F -labeled RGD and octreotide analogs. *J Nucl Med*. 2004;45:892–902.
11. Iwata R, Pascali C, Bogni A, et al. A new, convenient method for the preparation of 4- ^{18}F fluorobenzyl halides. *Appl Radiat Isot*. 2000;52:87–92.
12. Wilson A, Dannals R, Ravert H, Wagner H. Reductive amination of ^{18}F fluorobenzaldehydes: radiosyntheses of [2- ^{18}F]- and [4- ^{18}F]-fluorodexetimides. *J Labelled Comp Radiopharm*. 1990;28:1189–1199.
13. Tada M, Oikawa A, Iwata R, et al. An efficient, one-pot synthesis of 2-deoxy-2- ^{18}F fluoroacetamido-D-glucopyranose (N- ^{18}F fluoroacetyl-D-glucosamine), potential diagnostic imaging agent. *J Labelled Comp Radiopharm*. 1989; 27:1317–1324.
14. Wester HJ, Hamacher K, Stocklin G. A comparative study of N.C.A. fluorine-18 labeling of proteins via acylation and photochemical conjugation. *Nucl Med Biol*. 1996;23:365–372.
15. Marik J, Hausner SH, Fix LA, Gagnon MK, Sutcliffe JL. Solid-phase synthesis of 2- ^{18}F fluoropropionyl peptides. *Bioconjug Chem*. 2006;17:1017–1021.
16. Guhlke S, Wester HJ, Bruns C, Stocklin G. (2- ^{18}F fluoropropionyl-(D)phenyl)-octreotide, a potential radiopharmaceutical for quantitative somatostatin receptor imaging with PET: synthesis, radiolabeling, in vitro validation and biodistribution in mice. *Nucl Med Biol*. 1994;21:819–825.
17. Li ZB, Wu Z, Chen K, Chin FT, Chen X. Click chemistry for ^{18}F -labeling of RGD peptides and microPET imaging of tumor integrin $\alpha_v\beta_3$ expression. *Bioconjug Chem*. 2007;18:1987–1994.
18. Tewson T. Procedures pitfalls and solutions in the production of [^{18}F]2-deoxy-2-fluoro-D-glucose: a paradigm in the routine synthesis of fluorine-18 radiopharmaceuticals. *Nucl Med Biol*. 1989;16:533–551.
19. Kilbourn M, Brodack J, Chi D, et al. [^{18}F]fluoride ion: a versatile reagent for radiopharmaceutical syntheses. *J Labelled Comp Radiopharm*. 1986;23:1174–1176.
20. Martin RB. Ternary complexes of Al^{3+} and F^- with a third ligand. *Coord Chem Rev*. 1996;141:23–32.
21. Karacay H, McBride W, Griffiths G, et al. Experimental pretargeting studies of cancer with a humanized anti-CEA x murine bispecific antibody construct and a $^{99\text{m}}\text{Tc}^{188}\text{Re}$ -labeled peptide. *Bioconjug Chem*. 2000;11:842–854.
22. Sharkey RM, Karacay H, Litwin S, et al. Improved therapeutic results by pretargeted radioimmunotherapy of non-Hodgkin's lymphoma with a new recombinant, trivalent, anti-CD20, bispecific antibody. *Cancer Res*. 2008;68: 5282–5290.
23. Gold DV, Goldenberg D, Karacay H, et al. A novel bispecific, trivalent antibody construct for targeting pancreatic carcinoma. *Cancer Res*. 2008;68:4819–4826.
24. Sharkey RM, Cardillo T, Rossi E, et al. Signal amplification in molecular imaging by pretargeting a multivalent, bispecific antibody. *Nat Med*. 2005;11: 1250–1255.
25. Goldenberg DM, Sharkey R, Paganelli G, et al. Antibody pretargeting advances cancer radioimmunodetection and radioimmunotherapy. *J Clin Oncol*. 2006; 24:823–834.
26. McBride WJ, Zanzonico P, Sharkey RM, et al. Bispecific antibody pretargeting PET (immunoPET) with an ^{124}I -labeled hapten-peptide. *J Nucl Med*. 2006; 47:1678–1688.
27. Sharkey RM, Karacay H, Vallabhajosula S, et al. Metastatic human colonic carcinoma: molecular imaging with pretargeted SPECT and PET in a mouse model. *Radiology*. 2008;246:497–507.
28. Rossi EA, Goldenberg DM, Cardillo TM, McBride WJ, Sharkey RM, Chang CH. Stably tethered multifunctional structures of defined composition made by the dock and lock method for use in cancer targeting. *Proc Natl Acad Sci USA*. 2006;103:6841–6846.
29. McBride WJ, Hansen HJ, Chang C-H, et al., inventors; Immunomedics, Inc., assignee. Methods and compositions for administering therapeutic and diagnostic agents. U.S. patent application US 2004/0241158 A1. December 2, 2004.
30. McBride WJ, Goldenberg DM, inventors; Immunomedics, Inc., assignee. Methods and compositions for improved F-18 labeling of proteins, peptides and other molecules. U.S. patent application 20080170989 A1. July 17, 2008.
31. Kim HW, Jeong JM, Lee Y-S, et al. Rapid synthesis of [^{18}F]FDG without an evaporation step using an ionic liquid. *Appl Radiat Isot*. 2004;61:1241–1246.
32. Boden V, Colin C, Barbet J, Le Doussal JM, Vijayalaxhmi M. Preliminary study of the metal binding site of an anti-DTPA-indium antibody by equilibrium binding immunoassays and immobilized metal ion affinity chromatography. *Bioconjug Chem*. 1995;6:373–379.
33. Martin RB. Ternary hydroxide complexes in neutral solutions of Al^{3+} and F^- . *Biochem Biophys Res Commun*. 1988;155:1194–1200.
34. Andre JP, Macke H, Kaspar A, Kunnecke B, Zehnder M, Macko L. In vivo and in vitro ^{27}Al NMR studies of aluminum(III) chelates of triazacyclononane polycarboxylate ligands. *J Inorg Biochem*. 2002;88:1–6.
35. Li L. The biochemistry and physiology of metallic fluoride: action, mechanism, and implications. *Crit Rev Oral Biol Med*. 2003;14:100–114.
36. Antony B, Chabre M. Characterization of the aluminum and beryllium fluoride species which activate transducin: analysis of the binding and dissociation kinetics. *J Biol Chem*. 1992;267:6710–6718.
37. Franke WG, Hennig K, Woller P, Hilbert K. Production and suitability of F 18-sodium hexafluoroaluminate for bone scintigraphy [in German]. *Radiobiol Radiother (Berl)*. 1972;13:533–542.
38. Scheinberg DA, Strand M, Gansow O. Tumor imaging with radioactive metal chelates conjugated to monoclonal antibodies. *Science*. 1982;215:1511–1513.